JOURNAL OF APPLIED POLYMER SCIENCE VOL. 16, PP. 811–833 (1972)

Rate of Emulsion Polymerization of Styrene

MAKOTO HARADA,* MAMORU NOMURA, HIDEKI KOJIMA,† WATARU EGUCHI,* and SHINJI NAGATA, *Department of Chemical Engineering, Kyoto University, Kyoto, Japan*

Synopsis

In emulsion polymerization, the Smith and Ewart theory gives about two or three times the number of polymer particles obtained by experiment. In this paper, a reaction model is proposed which, from the standpoint of reactor design, can give an adequate explanation of the whole course of an emulsion polymerization of monomer highly insoluble in water. Among other things, the generating process of polymer particles is examined in detail. It is demonstrated experimentally that a new parameter proposed here, which represents the degree of difficulty of monomer initiation in micelles, is indispensable in explaining that process. Also confirmed is that monomer initiation takes place more easily in polymer particles than in micelles. According to the new model, the progress of polymerization, i.e., monomer conversion, the number of the polymer particles, and properties of polymer thus produced can be estimated with satisfactory accuracy. Furthermore, approximate equations are derived for easier estimation.

INTRODUCTION

Emulsion polymerization is a kind of heterogeneous reaction where the number of polymer particles generated in the course of the reaction is closely connected with the progress of polymerization. For this reason, the mechanism of the reaction is very complex and there are a great deal of problems in the industrial operation of emulsion polymerization. It is considered that these problems cannot be solved without clarifying the reaction mechanism and reaction rate.

Smith and Ewart[1] proposed a quantitative theory for emulsion polymerization of highly water-insoluble monomers on the basis of Harkins' qualitative theory.[2] It has been generally supported by most researchers that their theory was reasonable. Recently, Roe[3] discussed the generating process of polymer particles in detail and pointed out that minute experiments and further research should be made to clarify the mechanism of emulsion polymerization of several monomers. In this paper, the authors discuss the reaction mechanism, bringing into focus the generating process of polymer particles, and establish from the standpoint of reactor design a model which can describe the whole course of emulsion polymerization of highly insoluble monomers.

* Present address: Engineering Research Institute, Kyoto University, Uji, Japan.
† Present address: Mitzubishi Rayon Company, Otake, Japan.

EXPERIMENTAL

Emulsion polymerizations were carried out in a reactor as shown in Figure 1. The reactor was a cylindrical glass vessel with a dished bottom. Four baffle plates were located at 90° intervals, and a four-bladed turbine-type impeller was employed. Dimensions of the reactor and the impeller are shown in Figure 2. Styrene monomer was distilled twice under vacuum (20 mm Hg), stored at −20°C under a nitrogen atmosphere and distilled under vacuum again before use. Water used was purified by distillation in an alkaline potassium permanganate solution. Sodium lauryl sulfate and potassium persulfate of extra-pure grade were used without further purification as emulsifier and initiator, respectively. Before polymerization was started, water, emulsifier, and monomer were fed to the reactor, and the dissolved oxygen in these materials was removed by bubbling nitrogen gas through the mixture for $^1/_2$ hr. The nitrogen was deoxygenized by passing it through an alkaline pyrogallol solution and then an electrical furnace containing copper gauze at about 500°C. The aqueous initiator solution, which was also deoxygenized with the above gas, was then fed to the reactor and polymerization was started. The reaction temperature was maintained at 50°C by mean of a constant-temperature bath, and the impeller

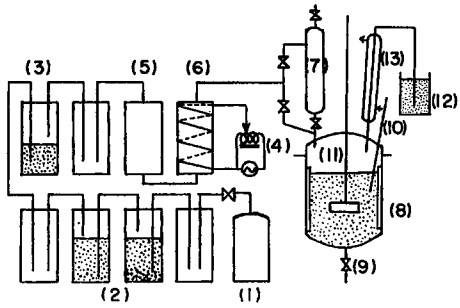

Fig. 1. Schematic diagram of experimental apparatus: (1) N_2 gas cylinder; (2) pyrogallol solution; (3) H_2SO_4; (4) voltage regulator; (5) $CaCl_2$; (6) electric furnace; (7) feeder for aqueous initiator solution; (8) reaction vessel; (9) sampling cock; (10) thermometer; (11) impeller; (12) pressure regulator; (13) reflux condenser.

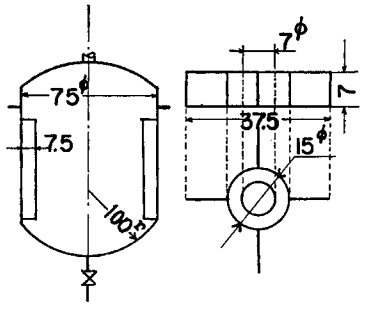

Fig. 2. Details of reaction vessel and impeller.

speed was kept constant at 400 rpm. Monomer conversion was determined gravimetrically, and the average degree of polymerization was determined by the viscosity-in-toluene-solution method, employing the Goldberg's equation.[4] The number of polymer particles was determined from the monomer conversion and the volume average diameter of polymer particles measured by an electron microscope. After separating the remaining monomer droplets in the sample with a centrifuge, the monomer concentration in the polymer particles was measured by weighing the polymer before and after polymerizing the residual monomer in the polymer particles. To follow the progress of polymerization, the surface tension of the aqueous phase free of monomer droplets was also measured by a du-Nöuy tensiometer.

RESULTS AND DISCUSSION

Characteristics of Emulsion Polymerization of Styrene

To clarify the mechanism of the emulsion polymerization of styrene, it is essential to known in detail the characteristic features of the reaction. For this purpose, the monomer conversion X_M, the average degree of polymerization $\bar{P}_\mu$, the surface tension of the aqueous phase σ, the number of polymer particles N_T, and monomer weight fraction in polymer particles ϕ were all measured during the polymerization.

One example of the experimental results is shown in Figure 3. The rate of polymerization r_{pc} (slope of X_M-vs.-t curve) increases gradually with reaction time t in the range $X_M < 0.146$, reaching a nearly constant value in the range $0.146 < X_M < 0.43$ and gradually decreasing in the range $X_M > 0.43$. The surface tension σ remains constant while the rate of polymerization is increasing; but when the rate reaches a constant value, corresponding to the time t_{c1}, the surface tension begins to increase sharply. Furthermore, the number of polymer particles increases with reaction time

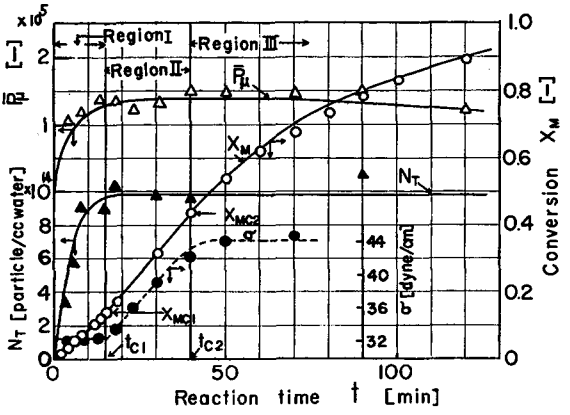

Fig. 3. Typical course of emulsion polymerization. Experimental condition, I_0 = 1.25 g/l. water, M_0 = 0.50 g/cc water, and S_i = 25.0 g/l. water.

t up to t_{c1}. These experimental results are considered to correspond to the assumption that the polymer particles are generated from emulsifier micelles, as pointed out by Harkins.[2] In this paper, the range $t < t_{c1}$, or $X_M < X_{Mc1}$, is called region I, where the conversion X_{Mc1} corresponds to the reaction time t_{c1}. Figure 4 shows the weight fraction of monomer in the polymer particles, ϕ. The value of ϕ is nearly constant in the range $X_M < 0.43$, and the variation of ϕ with conversion X_M is expressed by the equation $\phi = 1 - X_M$ in the range $X_M > 0.43$. These experimental results indicate that monomer droplets exist in the range $X_M < 0.43$, while in the range $X_M > 0.43$, the number of polymer particles and the total volume of polymer particles remain almost constant. Hence, the surface tension remains unaltered. If X_{Mc2} and t_{c2}, denote respectively, the conversion and the time at which the monomer droplets just disappear, the ranges $X_{Mc1} < X_M < X_{Mc2}$ and $X_M > X_{Mc2}$ can be designated as region II and region III, respectively. The critical conversion X_{Mc1} and time t_{c1} obtained at several reaction conditions are shown in Figure 5. The critical conversion X_{Mc2} is given by eq. (1) independently of the emulsifier concentration initially charged, S_i, as can be seen in Figure 4:

$$X_{Mc2} = 0.43. \tag{1}$$

As shown in Figure 6, the rate of polymerization r_{pc} in region II is nearly constant, regardless of the reaction time t, and is proportional to the number of polymer particles N_{Tc}. This result appears to support the validity of the Smith and Ewart theory,

$$r_{pc} = k_p M_{pc} N_{Tc}/2, \tag{2}$$

where k_p denotes the reaction rate constant of propagation and M_{pc} is the monomer concentration in the polymer particles in region II. M_{pc} has the following value:

$$M_{pc} = 5.48 \text{ g-moles/liter}. \tag{3}$$

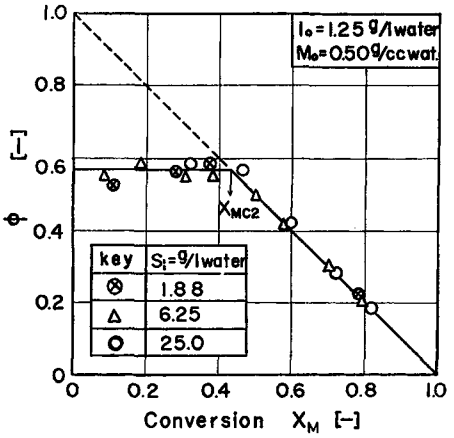

Fig. 4. Relationship between monomer conversion and monomer weight fraction in monomer-swollen polymer particles.

Proposed Reaction Model and Rate of Polymerization

From the experimental results and arguments presented above, a kinetic model can be developed, as shown in Table I, with the assumption that there is not more than one radical in each polymer particle.

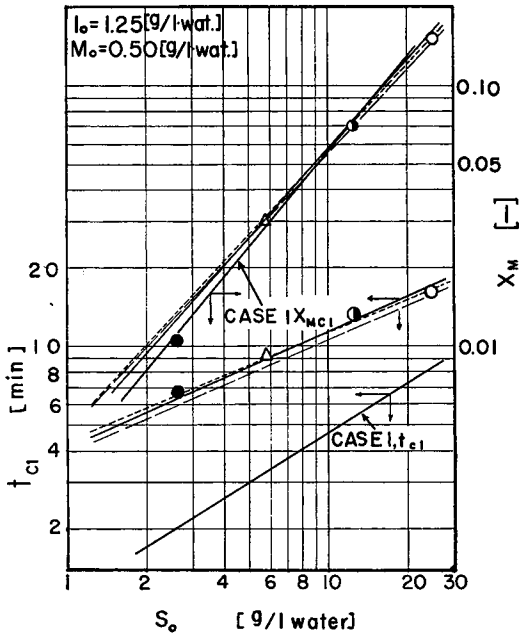

Fig. 5. Comparison of observed and calculated values of X_{Mc1} and t_{c1}: solid line, exact numerical calculation with $\epsilon = 1.28 \times 10^5$; broken line, approximate calculation with $\epsilon = 1.28 \times 10^5$; dotted line, approximate calculation with $\epsilon = 1.68 \times 10^5$.

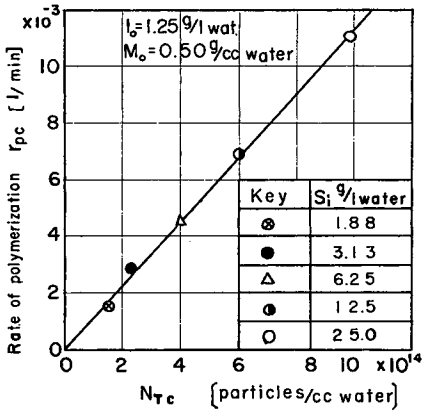

Fig. 6. Relationship between rate of polymerization and number of polymer particles.

TABLE I
Elementary Reactions of Emulsion Polymerization and Their Rates

Reaction	Reaction type	Reaction rate
Initiator decomposition	$I \rightarrow 2R^*$	$r_i = 2k_d f I_0$ (A)
Formation of particles	$R^* + m_s \rightarrow N^*$	$k_1 m_s R^*$ (B)
Initiation	$N + R^* \rightarrow N^*$	$k_2 N R^*$ (C)
Termination	$N^* + R^* \rightarrow N$	$k_2 N^* R^*$ (D)
Propagation in particle	$P^*_j + M \rightarrow P^*_{j+1}$	$k_p M_p N^*$ (E)
Transfer to monomer	$P^*_j + M \rightarrow M^* + P_j$	$k_{fm} M_p N^*$ (F)
Transfer to transfer agent	$P^*_j + T \rightarrow T^* + P_j$	$k_{fT} M_p N^*$ (G)

According to this model, the following equations are obtained for the respective materials:
Initiator radicals:

$$\frac{dR^*}{dt} = r_i - k_1 m_s R^* - k_2 N_T R^* \tag{4}$$

where

$$r_i = 2k_d f I_0. \tag{5}$$

In this experiment, it is reasonable to assume that r_i is constant because the half-life of the decomposition of potassium persulfate is sufficiently long compared with the whole reaction time.

Applying the stationary-state method to evaluate the concentration of the initiator radicals, the following equations may be derived:

$$R^* = r_i/(k_1 m_s + k_2 N_T) \tag{6}$$

Total number of polymer particles:

$$\frac{dN_T}{dt} = k_1 m_s R^*. \tag{7}$$

Substituting eq. (6) in eq. (7) yields

$$\frac{dN_T}{dt} = \frac{r_i}{1 + k_2 N_T/k_1 m_s} = \frac{r_i}{1 + \epsilon N_T/S} \tag{8}$$

where $\epsilon = k_2 M_m/k_1$ and M_m is the aggregation number of a micelle. The term $k_2 N_T/k_1 m_s$ represents the ratio of radical entry into a micelle and a polymer particle. Hence, ϵ is a kind of effectiveness factor for the particles relative to micelles in collecting an initiator radical and is an important factor in developing the model hereafter.

The number of active polymer particles N_j^* which have a polymer radical containing j units is obtained as follows:

$$\frac{dN_1^*}{dt} = k_1 m_s R^* - k_p M_p N_1^* + k_2 N R^* - k_2 N_1^* R^* + k_{fm} M_p N^* - k_{fm} M_p N_1^* + k_{fT} T_p N^* - k_{fT} T_p N_1^* \tag{9}$$

$$\frac{dN_j^*}{dt} = k_p M_p N^*_{j-1} - k_p M_p N_j^* - k_2 N_j^* R^* - (k_{fm} M_p + k_{fT} T_p) N_j^*. \quad (10)$$

Total active polymer particles:

$$\frac{dN^*}{dt} = k_1 m_s R^* + k_2 (N_T - 2N^*) R^* = r_i \left(1 - \frac{2N^*}{N_T + S/\epsilon}\right) \quad (11)$$

where

$$N^* = \sum_{j=1}^{\infty} N_j^* \quad (12)$$

$$N_T = N + N^* \quad (13)$$

Dead polymer:

$$\frac{dP_j}{dt} = k_2 N_j^* R^* + (k_{fm} M_p + k_{fT} T_p) N_j^* \quad (14)$$

Polymerization rate:

$$\frac{dX_M}{dt} = \left(\frac{k_p M_p M_w}{M_0 N_A}\right) N^* = \left(K \frac{M_p}{M_{pc}}\right) N^* \quad (15)$$

where

$$K = \frac{k_p M_{pc} M_w}{M_0 N_A} \quad (16)$$

Emulsifier micelles:

The depletion of emulsifier micelles occurs because they break up and their molecules are adsorbed on the surface of growing polymer particles. Provided that the emulsifier molecules are adsorbed in a monomolecular layer on the surface of the polymer particles and that the dissociation of emulsifier micelles and the adsorption of emulsifier molecules are very rapid compared to the rates of the other processes, the following equation may be obtained:

$$S = S_0 - k_v (M_0 X_M)^{2/3} N_T^{1/3} \quad (17)$$

where

$$k_v = [36\pi/(1 - \phi_c)^2 a_s^3 \rho^2]^{1/3} \quad (18)$$

and S_0 denotes the concentration of the emulsifier effective in the initiation of micelles, i.e., $S_0 = S_t - S_{CMC}$. (The critical micelle concentration, S_{CMC}, was 0.50 g/l. at 50°C at these experimental conditions.)

Considering the results of many investigators, the generating process of polymer particles is the most obscure one among the various processes involved in emulsion polymerization. In particular, the generating process of polymer particles is considered to be greatly influenced by the value of ϵ, but the effect of ϵ upon that process cannot be clarified analytically since a

general analytical solution of the set of eqs (4) to (18) is not obtainable. Hence, let us consider initially the two limiting cases which can describe analytically the characteristic features of emulsion polymerization, especially the generating process of the polymer particles.

One is the case satisfying the condition $\epsilon N_T/S \ll 1$ where the initiator radicals generated in the aqueous phase enter preferentially into the micelles rather than into the polymer particles. The other is the case of $\epsilon N_T/S \gg 1$, which is exactly opposite to the above case. These two cases illustrate different features of the generation process of polymer particles and are useful for understanding the process of emulsion polymerization and determining the parameters in the model.

Case 1: $\epsilon N_T/S \ll 1$

This corresponds to the first idealized situation of Smith and Ewart.[1] In this case, eqs. (7) and (11) in region I may be simplified:

$$N_T = N^* = r_i t. \tag{19}$$

From eqs. (15) and (19), monomer conversion X_M in region I is given as follows:

$$X_M = \frac{K}{2} r_i t^2. \tag{20}$$

The critical time t_{c1} and conversion X_{Mc1} where the emulsifier micelles disappear and the generation of polymer particles ceases are given as follows:

$$t_{c1} = \left(\frac{KM_0}{2}\right)^{-2/5} \left(\frac{S_0}{r_i k_v}\right)^{2/5} \tag{21}$$

$$X_{Mc1} = \left(\frac{K}{2r_i}\right)^{1/5} \left(\frac{S_0}{k_v}\right)^{6/5} (M_0)^{-4/5}. \tag{22}$$

The number of polymer particles is evaluated by eqs. (17), (21), and (22) after the micelles disappear:

$$N_{Tc} = \left(\frac{2r_i}{M_0 K}\right)^{2/5} \left(\frac{S_0}{k_v}\right)^{3/5}. \tag{23}$$

In region II, the number of active polymer particles is given by the following equation:

$$N^* = \frac{N_{Tc}}{2}\left[1 + \exp\left\{-\frac{2(t - t_{c1})}{t_{c1}}\right\}\right]. \tag{24}$$

The conversion of monomer X_M in region II is calculated from eqs. (15) and (24):

$$X_M - X_{Mc1} = \frac{KN_{Tc}}{2}\left[t - t_{c1} - \frac{t_{c1}}{2}\exp\left\{-\frac{2(t - t_{c1})}{t_{c1}}\right\}\right]. \tag{25}$$

Although the number-average degree of polymerization can be calculated from eqs. (7) to (14), the solution cannot be obtained easily because the stationary-state method is not applicable in the range of region I and in the early stage of region II. However, for $t > t_{c1}$, N^* rapidly approaches the value $N_T/2$, and the stationary state method is applicable to active polymer particles. The number-average degree of polymerization of the polymer produced after the attainment of the stationary state is given by eq. (26). The number-average degree of polymerization of the polymer formed in region II can be approximately estimated by eq. (26) because the amount of the polymer formed in region I and in the early stage of region II is generally much smaller than the total polymer formed in region II:

$$\bar{P}_{Nc} = \frac{k_p M_{pc} N_{Tc}}{r_i + [k_{fm} M_{pc} + k_{fT} T_p] N_{Tc}} \tag{26}$$

In region III, monomer conversion X_M is given as follows, with the assumption that the density of polymer particles remains unaltered as the polymerization progresses:

$$\ln \frac{1 - X_{Mc2}}{1 - X_M} = \frac{K N_{Tc}}{2(1 - X_{Mc2})} \left[(t - t_{c2}) - \frac{t_{c1}}{2} \left[\exp\left\{ - \frac{2(t - t_{c1})}{t_{c1}} \right\} - \exp\left\{ - \frac{2(t_{c2} - t_{c1})}{t_{c1}} \right\} \right] \right]. \tag{27}$$

As $t > t_{c2} \gg t_{c1}$ usually holds, eq. (27) may be substituted by the following one without loss of accuracy:

$$\ln \frac{1 - X_{Mc2}}{1 - X_M} = \frac{K N_{Tc}}{2(1 - X_{Mc2})} (t - t_{c2}). \tag{27'}$$

Case 2: $\epsilon N_T/S \gg 1$

This means that almost all the initiator radicals generated in the aqueous phase are captured by the polymer particles present. Therefore, the following equations* will be valid from the very beginning to the end of the reaction:

$$N^* = N = \frac{N_T}{2}. \tag{28}$$

The amount of emulsifier remaining as micelles at time t in the aqueous phase is approximately given by the following equation:

$$S = S_0 \left(1 - \frac{t}{t_{c1}} \right). \tag{29}$$

* The validity of the assumption in eqs. (28) and (29) was verified by numerical calculations with a digital computer and is explained in the Appendix.

From eqs. (7) and (29), the generation rate of polymer particles is given as follows:

$$\frac{dN_T}{dt} = \left(\frac{r_i S_0}{\epsilon N_T}\right)\left(1 - \frac{t}{t_{c1}}\right). \tag{30}$$

Integration of eq. (30) leads to eq. (31):

$$N_T = \left(\frac{r_i S_0}{\epsilon}\right)^{1/2}\left(2t - \frac{t^2}{t_{c1}}\right)^{1/2}. \tag{31}$$

From eqs. (15), (28), and (31), monomer conversion X_M in region I is derived as follows:

$$X_M = \frac{K}{4} t_{c1}^{3/2}\left(\frac{r_i S_0}{\epsilon}\right)^{1/2}\left[\cos^{-1}\left(1 - \frac{t}{t_{c1}}\right) - \left(1 - \frac{t}{t_{c1}}\right)\left\{1 - \left(1 - \frac{t}{t_{c1}}\right)^2\right\}^{1/}\right]. \tag{32}$$

From eqs. (17), (31), and (32), the critical values of t_{c1} and X_{Mc1} are given as follows:

$$t_{c1} = k_v^{-6/7}\left(\frac{\pi K M_0}{8}\right)^{-4/7}\left(\frac{S_0\epsilon}{r_i}\right)^{3/7} \tag{33}$$

$$X_{Mc1} = k_v^{-9/7}\left(\frac{\pi K M_0}{8}\right)^{1/7}\left(\frac{\epsilon}{r_i}\right)^{1/7}(S_0)^{3/7} M_0^{-1}. \tag{34}$$

Substituting eq. (33) in eq. (31), the total number of polymer particles formed is given by eq. (35):

$$N_{Tc} = k_v^{-3/7}\left(\frac{\pi K M_0}{8}\right)^{2/7}\left(\frac{r_i}{\epsilon}\right)^{2/7} S_0^{5/7}. \tag{35}$$

Monomer conversion X_M in region II is obtained by eq. (36):

$$X_M = \frac{1}{2} K N_{Tc}(t - t_{c1}) + X_{Mc1}. \tag{36}$$

Monomer conversion X_M in region III may be expressed as follows, without taking into account the density change of the polymer particles:

$$\ln\frac{1 - X_{Mc2}}{1 - X_M} = \frac{K N_{Tc}}{2(1 - X_{Mc2})}(t - t_{c2}). \tag{37}$$

Let us consider the polymer properties estimated by this model. Chain-transfer agents, denoted by T, are neglected because their behavior is not clear in emulsion polymerization and they were not used in these experiments.

Applying the stationary-state method to eqs. (9) and (10) and considering the relations of eq. (28) and $\epsilon N_T/S \gg 1$, the number of active polymer particles containing a polymer radical with j units of monomer, N_j^*, is as follows:

$$N_j^* = \left(\frac{2k_1m_sR^* + k_{mf}M_pN_T}{2k_pM_p}\right)\exp\left\{-\frac{(r_t/N_T) + k_{mf}M_p}{k_pM_p}(j-2)\right\}. \quad (38)$$

Substituting eq. (38) in eq. (14) yields the following equation:

$$\frac{dP_j}{dt} = \left(\frac{2k_1m_sR^* + r_t + k_{mf}M_pN_T}{2k_pM_p}\right)\exp\left\{-\frac{(r_t/N_T) + k_{mf}M_p}{k_pM_p}(j-2)\right\} \quad (39)$$

where N_T is dependent on reaction time t only in region I, and M_p is dependent on t only in region III. The solution of eq. (39) gives the molecular weight distribution of polymer produced and the average degree of polymerization.

The definition of viscosity-average degree of polymerization is as follows:

$$\bar{P}_\mu = \left\{\frac{\sum_{j=1}^{\infty} j^{1+a}(P_j + N_j^*)}{\sum_{j=1}^{\infty} j(P_j + N_j^*)}\right\}^{1/a} \quad (40)$$

where a is the power number in the Mark-Houwink equation.

The viscosity-average degree of polymerization in region I is approximately given by the following equation, using the relations of eqs. (31), (39), and (40):

$$\bar{P}_{\mu I} = \frac{2\Gamma(a+2)\int_0^t \frac{\{k_pM_{pc}(2r_tS_0/\epsilon)^{1/2}(t - t^2/2t_{c1})^{1/2}\}^{a+1}}{\{r_t + k_{mf}M_{pc}(2r_tS_0/\epsilon)^{1/2}(t - t^2/2t_{c1})^{1/2}\}^{1/a}}\,dt}{k_pM_{pc}(2r_tS_0/\epsilon)^{1/2}[(t_{c1}^{3/2}/\sqrt{2})\{\pi/2 - \sin^{-1}(1 - t/t_{c1})\} - (t_{c1} - t)(t - t^2/2t_{c1})^{1/2}]}. \quad (41)$$

In region II, $\bar{P}_{\mu II}$ can be evaluated from eqs. (30) and (40):

$$\bar{P}_{\mu II} = \frac{k_pM_{pc}\Gamma(a+2)^{1/a}\left(\frac{2r_tS_0}{\epsilon}\right)^{(a+1)/2}}{N_{Tc}\{(\pi/4)t_{c1} + t - t_{c1}\}} \times \left[\int_0^{t_c} \frac{(t - t^2/2t_{c1})^{(a+1)/2}\,dt}{\{r_t + k_{mf}M_{pc}(2r_tS_0/\epsilon)^{1/2}(t - t^2/2t_{c1})^{1/2}\}^a} + \frac{N_{Tc}(t - t_{c1})}{(r_t/N_{Tc} + k_{mf}M_{pc})^a}\right]. \quad (42)$$

If $t \gg t_{c1}$, eq. (42) leads approximately to eq. (43):

$$\bar{P}_{\mu c} = \bar{P}_{\mu II} = \Gamma(a+2)^{1/a}\frac{k_pM_{pc}}{r_t/N_{Tc} + k_{mf}M_{pc}} \quad (43)$$

and

$$\bar{P}_{Nc} = \frac{k_pM_{pc}}{r_t/N_{Tc} + k_{mf}M_{pc}}. \quad (44)$$

In region III, $\bar{P}_{\mu III}$ is estimated by eq. (45):

$$\bar{P}_{\mu III} = \frac{k_p M_{pc}\,\Gamma\,(a+2)^{1/a}}{N_{Tc}\{(\pi/4)t_{c1} - t_{c1} + t_{c2}\} + (2/K)(X_M - X_{Mc2})} \times \left[\left(\frac{2r_i S_0}{\epsilon}\right)^{(a+1)/2} \int_0^{t_{c1}} \frac{(t - t^2/2t_{c1})^{(a+1)/2}\,dt}{\left\{r_i + k_{mf} M_{pc} \left(\frac{2r_i S_0}{\epsilon}\right)^{1/2} (t - t^2/2t_{c1})^{1/2}\right\}^a} + \frac{N_{Tc}^{a+1}(t_{c2} - t_{c1})}{(r_i + k_{mf} M_{pc} N_{Tc})^a} + \left(\frac{N_{Tc}}{1 - X_{Mc2}}\right)^{a+1} + \int_{t_{c2}}^{t} \frac{(1 - X_M)^{a+1}\,dt}{r_i + k_{mf} M_{pc} N_{Tc}(1 - X_M)/(1 - X_{Mc2})^a} \right] \quad (45)$$

Consideration of Parameters and Generating Mechanism of Polymer Particles

Let us consider the difference in the expressions of the progress of the reaction between case 1 and 2. In region II, monomer conversion X_M is expressed by eq. (36) when $\epsilon N_T/S \gg 1$. In other words, X_M varies linearly with reaction time t, while in the case of $\epsilon N_T/S \ll 1$, X_M is expressed by eq. (25). Since the conversion predicted by eq. (25) coincides approximately with that calculated by eq. (36) if $t/t_{c1} > 3$, the parameter K can be evaluated by eqs. (25) and (36) regardless of $\epsilon N_T/S$, as long as the condition $t/t_{c1} > 3$ is satisfied. In region III, the value of K calculated by eq. (27) also coincides approximately with that calculated by eq. (37). Therefore, the value of K was evaluated by eqs. (36) and (37) together with the terms X_M, X_{Mc1}, and X_{Mc2}. This result is shown in Figure 7. K remains at a constant value independently of the initial emulsifier concentration S_i at low conversions, but deviates from this constant value at comparatively high conversions. The deviation becomes greater as the emulsifier concentration decreases, or in other words, the volume of the polymer particles

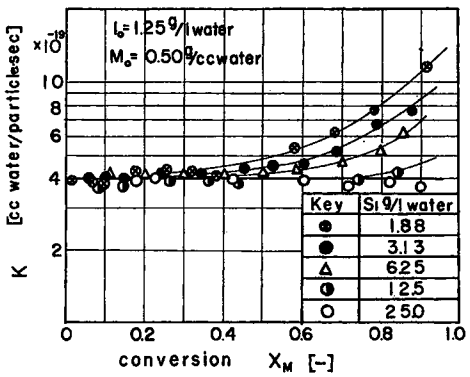

Fig. 7. Relationship between the value of K and monomer conversion.

increases. The deviation of K from the constant value seems, as pointed out by Stockmayer,[5] to be attributed to the so-called autoacceleration effect. Neglecting autoacceleration, the value of K becomes:

$$K = 4.0\times10^{-19} \text{ cc water/particle·sec.} \tag{46}$$

From the values of K and M_{pc} at 50°C, k_p can be calculated:

$$k_p = 212 \text{ l./g-mole·sec.} \tag{47}$$

This value agrees well with those reported (Olive,[6] 209 l./g-mole·sec; Bartholome,[7] 223 l./g-mole·sec at 50°c).

The average degree of polymerization in region II may be evaluated approximately by eq. (44) independently of $\epsilon N_T/S$. Rearranging eq. (44) leads to the following equation:

$$\frac{1}{\bar{P}_{Nc}} = \frac{k_{mf}}{k_p} + \left(\frac{2k_df}{k_pM_{pc}}\right)\left(\frac{I_0}{N_{Tc}}\right). \tag{48}$$

The viscosity-average degree of polymerization $\bar{P}_{\mu c}$ was converted to $\bar{P}_{Nc}$ by eqs. (43) and (44), and the reciprocal of the number-average degree of polymerization, $1/\bar{P}_{Nc}$, is plotted against (I_0/N_{Tc}) in Figure 8. The symbols (●), (△), and (⊙) indicate the experimental results obtained at the reaction conditions I_0 = 1.25 g/l. water and S_t = 1.88, 6.25, and 25.0 g/l. water, while the symbol (⊗) shows the results obtained when the seed of polymer particles was prepared at I_0 = 1.25 g/l. water, S_t = 1.88 g/l. water, and a specified quantity of initiator was added to the reaction mixture. (More initiator was added as soon as the generation of seed particles ceased, so any polymer formed before that addition was negligible.) The number-average degree of polymerization in region II satisfies eq. (44), so k_df can be predicted as follows:

$$k_df = 6.65\times10^{-7} \text{ 1/sec at 50°C.} \tag{49}$$

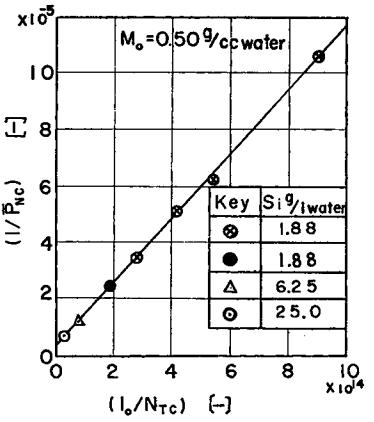

Fig. 8. Plot of $1/\bar{P}_{Nc}$ vs. I_0/N_{Tc}.

TABLE II
Values of (r_i/ϵ), K, and k_v in Region I

Initial soap concentration S_i, g/l.	r_i/ϵ, 1/sec	K, cc/ particle·sec	k_v
3.13	2.64×10^{7}	2.4×10^{-19}	3.09×10^{15}
6.25	2.31×10^{7}	3.6×10^{-19}	2.67×10^{15}
12.5	2.23×10^{7}	3.1×10^{-19}	2.70×10^{15}
25.0	2.28×10^{7}	3.8×10^{-19}	2.87×10^{15}

The value of $k_d f$ obtained above agrees well with the value of the potassium persulfate decomposition rate constant given in the literature (Kolthoff et al.,[8] 10.0×10^{-7} 1/sec at 50°C).

The value of k_v is also independent of $\epsilon N_T/S$ and can be evaluated from eq. (17) with the values of X_{Mc1} from Figure 5 and N_{Tc} from Figure 11.

The value of k_v remains almost constant regardless of the initial emulsifier S_i, as shown in Table II. The value of a_s, the area per emulsifier molecule, calculated from k_v is given as follows:

$$a_s = 35 \times 10^{-16} \text{ cm}^2/\text{molecule}. \tag{50}$$

This value agrees approximately with literature values for adsorption at oil/water interface of 45–50 Å^2. As mentioned above, the values of K, $k_d f$, and k_v predicted from experimental data in region II are independent of $\epsilon N_T/S$ as long as the experimental value of N_{Tc} is used. On the other hand, in region I, the progress of the reaction is greatly influenced by the value of $\epsilon N_T/S$ because new polymer particles are being generated in this region. In the case of $\epsilon N_T/S \ll 1$, the conversion X_M is a function of t, K, and r_i, while if $\epsilon N_T/S \gg 1$, X_M is a function of t, K, r_i, and S_0. Figure 9 shows the observed variation of monomer conversion with reaction time in region I.

The broken line in Figure 9 represents the progress of polymerization in the early stages, which was estimated by eq. (20) with the values of eqs. (46) and (49). The experimental data points are greatly influenced by the value of S_0 and cannot be explained by the broken line, but when the data are rearranged as in Figure 10 according to the terms in eq. (32), it is clear that experimental observations satisfy eq. (32).

The values of (r_i/ϵ) and K in region I evaluated by eqs. (33) to (35) with the experimental values of X_{Mc1}, t_{c1}, and N_{Tc} are shown as a function of S_i in Table II. These values are nearly constant and independent of the initial emulsifier concentration S_i, and K takes almost the same value as obtained in region II. The above results are indicative that the emulsion polymerization proceeds approximately according to the case of $\epsilon N_T/S \gg 1$, and the mean value of (r_i/ϵ) predicted from the slope of the straight line in Figure 10 is almost equal to those mentioned in Table II above.

The value of ϵ evaluated by the approximate equations corresponding to the limiting case of $\epsilon N_T/S \gg 1$ is

$$\epsilon = 1.68 \times 10^{5}. \tag{51}$$

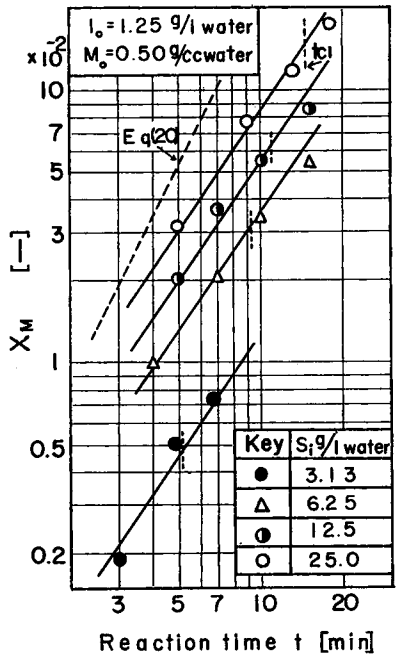

Fig. 9. Plot of monomer conversion vs. reaction time in region I.

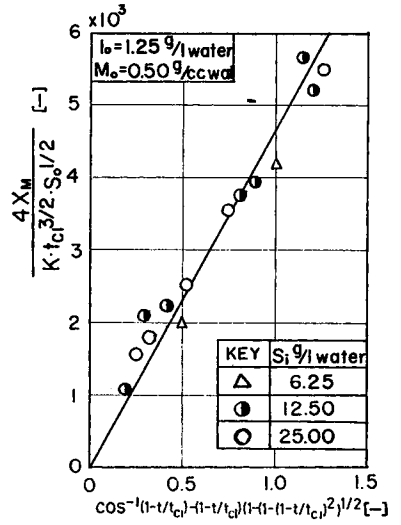

Fig. 10. Validity of case II in emulsion polymerization.

Strictly speaking, the value of ϵ should be predicted by solving the basic equations numerically so as to make the calculated value of N_T agree with the observed one. The final value is as follows:

$$\epsilon = 1.28 \times 10^5 \tag{52}$$

Comparison of Experimental and Calculated Results

As shown above, the experimental results could be explained by the basic equations. In particular, the course of emulsion polymerization of styrene could be followed approximately by eqs. (28) to (45) for the limiting case of $\epsilon N_T/S \gg 1$. Let us now compare the calculated values with those observed.

Generating Process of Polymer Particles

The variation of the number of polymer particles with reaction time in region I is shown in Figure 3 as an example. The solid line represents the results of an exact numerical solution of the basic equations by digital computer using the accurate value, $\epsilon = 1.28 \times 10^5$. These theoretical predictions are in good agreement with the experimental results.

Effect of Emulsifier Concentration of the Number of Polymer Particles

The effect of emulsifier concentration on the number of polymer particles formed is shown in Figure 11. The solid line shows the number of polymer particles estimated by solving the set of basic equations numerically. The dotted line is the one predicted by eq. (35) using the approximate value $\epsilon = 1.68 \times 10^5$. It is apparent that the estimations of the number of polymer particles by these two methods agree well with the experimental results.

Effects of Emulsifier, Initiator, and Monomer Concentration on Progress of Polymerization

A comparison of the progress of polymerization between calculation and experiment is shown in Figures 12, 13, and 14, where the solid lines represent the results of numerical calculation using the basic equations with $\epsilon = 1.28 \times 10^5$, and the broken lines, the results of an approximate estimation by the equations for the case of $\epsilon N_T/S \gg 1$ with $\epsilon = 1.28 \times 10^5$. The

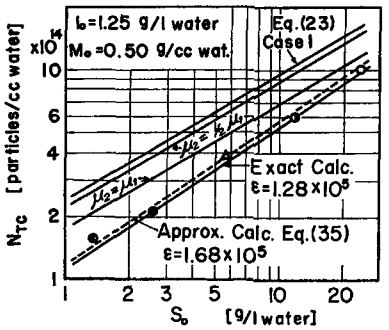

Fig. 11. Comparison of observed and calculated values of the number of polymer particles: solid line; exact numerical calculation with $\epsilon = 1.28 \times 10^5$; dotted line, approximate calculation with $\epsilon = 1.68 \times 10^5$.

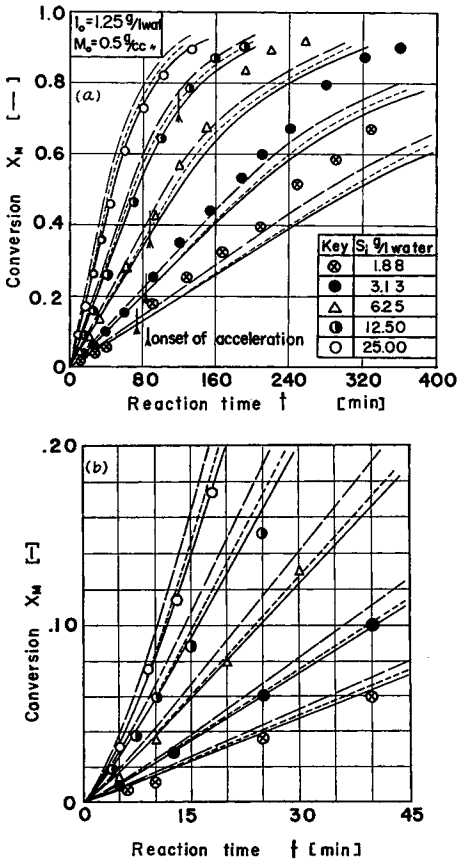

Fig. 12. Comparison of calculated conversion time curves with experimental data at various emulsifier concentrations.

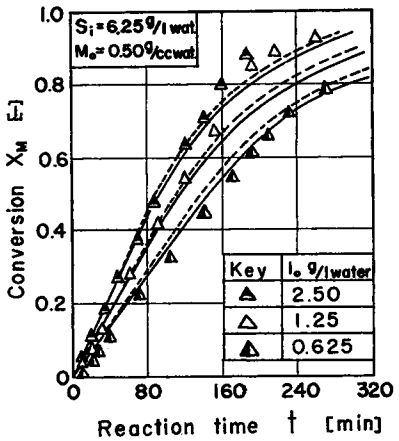

Fig. 13. Comparison of calculated conversion time curves with experimental data at various initiator concentrations.

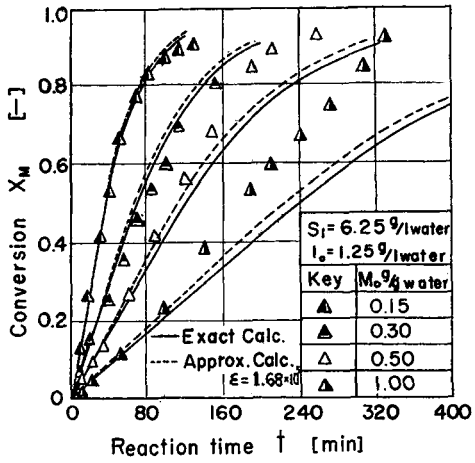

Fig. 14. Comparison of calculated conversion time curves with experimental data at various initial monomer concentrations.

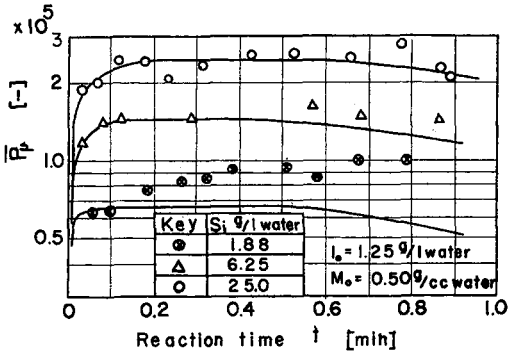

Fig. 15. Comparison of calculated $\bar{P}_\mu$ conversion curves with experimental data.

dotted lines represent the results of an approximate estimation by eqs. (28) to (45) for the case of $\epsilon N_T/S \gg 1$ with $\epsilon = 1.68 \times 10^5$.

As can be seen in Figures 12, 13, and 14, excellent quantitative agreement is obtained between the rigorous predictions represented by the solid lines and the observed values, except in the range where the autoacceleration effect occurs. Furthermore, the approximate prediction of the rate by the equations for the case of $\epsilon N_T/S \gg 1$ gives just as good a fit as the rigorous predictions given above as long as the value $\epsilon = 1.68 \times 10^5$ is used.

According to the approximate expression for the average degree of polymerization corresponding to the condition of $\epsilon N_T/S \gg 1$, the variation of the viscosity-average degree of polymerization $\bar{P}_\mu$ with monomer conversion can be easily calculated by eqs. (40) to (47). A comparison between the calculated and the observed values is shown in Figure 15. The deviation of the calculated values from those observed at comparatively high monomer conversions may be attributed to the autoacceleration effect. The degree of deviation becomes more marked as the initial emulsifier

concentration S_i decreases. This is due to the fact that the volume of particles increases because of the decrease in the number of polymer particles formed, so the autoacceleration effect becomes more marked.

DISCUSSION

Smith and Ewart proposed two idealized situations for the generating process of polymer particles, and their theory is related to our model as follows.

In the first idealized situation, it is supposed that the initiator radicals generated in the water phase are all captured by the micelles and do not enter the particles as long as the micelles are present. Then,

$$\epsilon = (k_2/k_1)M_m = 0. \tag{53}$$

The number of polymer particles produced in this situation is given by

$$N_T = 0.53\mu_1^{-2/5}r_i^{2/5}(a_sS_0)^{3/5}. \tag{54}$$

In the application of eq. (54), one should employ the following value as the average rate of volume increase per particle, μ_1, since in this situation, each particle has only one polymerizing radical as long as the micelles are present:

$$\mu_1 = k_pM_p \cdot 1 \cdot \frac{M_w}{N_A\rho(1 + \phi)} = \frac{KM_0}{\rho(1 - \phi_c)} \tag{55}$$

In the second idealized situation, it is supposed that a given interfacial area on the micelles and on the polymer particles always has the same effectiveness in collecting initiator radicals. Then ϵ is

$$\epsilon = (k_2/k_1)M_m = \left(\frac{d_p}{d_m}\right)^2 M_m \tag{56}$$

where d_m and d_p denote the average diameters of micelle and polymer particles, respectively. In this situation, the well-known expression for the number of polymer particles produced is given as follows:

$$N_T = 0.37\mu_2^{-2/5}r_i^{2/5}(a_sS_0)^{3/5}. \tag{57}$$

Since the initiator radicals enter the particles in proportion to the interfacial area of the particles, the average number of polymerizing radicals per particle range from one half to unity, tending much closer to the former. Then μ_2 is

$$\mu_1/2 < \mu_2 < \mu_1 \tag{58}$$

There exists an intermediate situation between the two idealized situations of Smith and Ewart. According to Fick's law, k_1 and k_2 obey the following relations, respectively:

$$\begin{aligned} k_1 &= 2\pi Dd_m \\ k_2 &= 2\pi Dd_p \end{aligned} \tag{59}$$

where D is the diffusion coefficient of initiator radicals in the water phase. In this case, ϵ is

$$\epsilon = k_2/k_1M_m = \left(\frac{d_p}{d_m}\right) \cdot M_m. \tag{60}$$

According to the study of the present paper, both the first idealized and the intermediate situation correspond to our case 1 because the conditions in these situations fulfill the inequality $\epsilon N_T/S \ll 1$. These situations give about twice the number of particles actually observed, as shown in Figure 11.

In the second idealized situation, the number of polymer particles predicted by eqs. (57) and (58), will lie between the two limiting lines ($\mu_2 = \mu_1$ and $\mu_2 = \mu_1/2$) in Figure 11 and will be much closer to the upper line ($\mu_2 = \mu_1/2$) since, as described above, the value of μ_2 is much closer to $\mu_1/2$ than it is to μ_1. Thus, the number of polymer particles in the second idealized situation is also about twice as much as the observed values.

Let us consider the reason for the above discrepancy in the number of polymer particles. The value of ϵ obtained by the experiments in this laboratory is 1.28×10^5. On the other hand, the value of ϵ estimated by eq. (56) is about the order of 10^4 because M_m is usually 10^2 for sodium lauryl sulfate in an electrolyte solution and the value of $(d_p/d_m)^2$ has an order of 10^2 at the most. Therefore, the above discrepancy arises because the initiator radicals have more difficulty in entering the micelles than supposed by Smith and Ewart. The difficulty of radical entry into the micelles may be due to the following two factors. One is that the energy barrier against the entry of the initiator radicals into the micelles and the polymer particles is different. The other is that the radicals, having entered the micelles, may escape again too rapidly to cause initiation because the micelle has too small a volume.

In the authors' opinion, the latter factor will play an important role not only in the process of particle formation but also in governing the polymerization rate per particle in the emulsion polymerization of several monomers. However, at the present stage, it is very difficult to estimate the energy barrier mentioned above, or to predict the rate constant of initiation in such a small reaction unit as a micelle.

The particle volume distribution is closely connected with the generating mechanism of the particles. The volume distribution at $X_M = 0.12$, the value of which is near the critical conversion $X_{Mc1} = 0.14$, is shown as an example in Figure 16. The absicca v is the volume of a particle, and the ordinate $f(v)$ is the probability density of particles with volume v. The volume distribution $f(v)$ for case 1 at conversion X_{Mc1} is easily evaluated:

$$f(v) = \begin{cases} 1/\mu_1 t_{c1} & v \leqq 1/\mu_1 t_{c1} \\ 0 & v > 1/\mu_1 t_{c1} \end{cases} \tag{61}$$

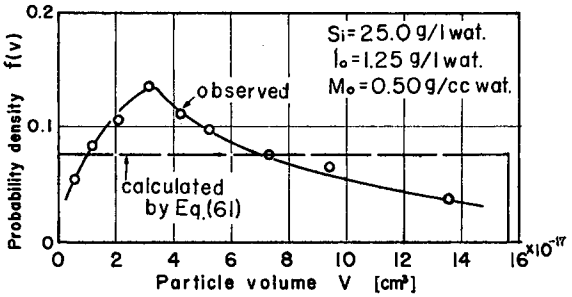

Fig. 16. Comparison of calculated and observed distributions.

The calculated distribution is represented by the broken line in Figure 16, but the observed distribution, on the other hand, is much sharper than that shown by the broken line. This means that at least the polymer particles do not form according to the mechanism of case 1. In the case of a large value of ϵ (case 2), the volume distribution $f(v)$ cannot be expressed in a simple form since the appearance or disappearance of initiator radicals in a particle is a complex probability process, but the process could be simulated by the Monte Carlo method.

A further discussion of the particle size distribution will be presented in a future paper.

CONCLUSIONS

The Smith and Ewart theory does not show good agreement with the experimental results in the generation process of polymer particles. The number of polymer particles predicted by their theory is about twice as much as that observed. According to the analysis in this paper, excellent quantitative agreement can be obtained between theoretical and experimental values of the number of polymer particles, the reaction rate, and the degree of polymerization. Therefore, the course of the reaction can be followed with adequate accuracy, except in the range where autoacceleration occurs. The effect of autoacceleration is very important in emulsion polymerization and may be estimated from the deviations from this reaction model. Quantitative studies on this effect will be reported in the near future. Discrepancy between the theoretical and the observed values of ϵ may provide a key for the understanding of the emulsion polymerization of several monomers, but a clear explanation cannot be given at the present moment.

Appendix

Equations (28) and (29) were derived approximately from the exact solutions of the basic equations (4) to (18), which were solved numerically with a digital computer. Part of the results of the numerical calculation is shown in Figure 17 and is compared with eqs. (28) and (29). It is concluded

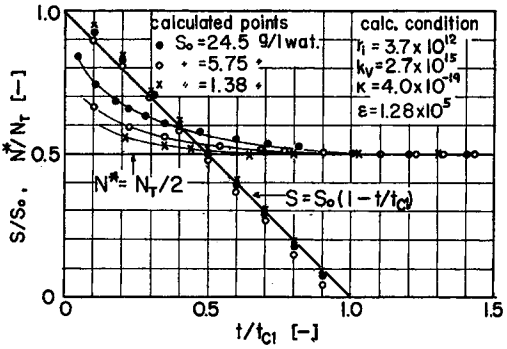

Fig. 17. Comparison of eqs. (28) and (29) with exact solutions.

that the validity of eq. (28) is reasonably good, except at the very beginning of the polymerization, and eq. (29) is a good approximation over the usual range of emulsifier and initiator concentrations.

Nomenclature

a = the power number in Mark-Houwink equation
a_s = surface area occupied by an emulsifier molecule, in cm²/molecule
D = diffusion coefficient of initiator radicals in aqueous phase, in cm²/sec
d_p = diameter of polymer particle, in cm
d_m = diameter of micelle, in cm
f = initiator efficiency
I = initiator concentration, in g/l. water or molecules/cc water
j = chain length of a polymer
k_v = $[36\pi/1(1-\phi_c)^2 a_s^3 \rho^2]^{1/3}$
k_1 = rate constant of formation of polymer particle defined by ev. (B), in cc water/molecule·sec
k_2 = rate constant defined by eqs. (C) and (D), in cc water/molecule·sec
k_d = decomposition rate constant of initiator, in [l./sec]
k_{fm} = transfer rate constant to monomer, in l./g-mole·sec
k_{ft} = transfer rate constant to transfer agent, in l./g-mole·sec
k_p = propagation rate constant, in l./g-mole·sec
M = monomer concentration, in g/cc water
M_p = monomer concentration in polymer particle, in g-mole/l.
M_m = aggregation number of micelle
M_w = molecular weight of monomer, in g/g-mole
m_s = emulsifier micelle concentration, in molecule/cc water
N = number of dead polymer particles, in particles/cc water
N^* = number of active polymer particles, in particles/cc water
N_j^* = number of particles containing a polymer radical with j monomer units, in particles/cc water
N_T = total number of polymer particles, in particles/cc water

N_A = Avogadro's number, in molecules/g-mole
P_j = dead polymer containing j units, in molecules/cc water
P_j^* = active polymer containing j units, in molecules/cc water
$\bar{P}_N$ = number-average degree of polymerization
$\bar{P}_\mu$ = viscosity-average degree of polymerization
R^* = concentration of initiator radical in the water phase, in molecules/cc water
r_i = generation rate of initiator radical, in molecules/cc water·sec
r_{pc} = polymerization rate in region II, in molecules/cc water·sec
S = emulsifier concentration effective for micelle formation, in g/l. or molecules/cc water
S_{CMC} = critical micelle concentration of the emulsifier, in molecules/cc water or g/l. water
S_i = concentration of emulsifier charged initially, in g/l. water or molecules/cc water
S_0 = $S_i - S_{CMC}$, in g/l. water or molecules/cc water
T_p = concentration of transfer agent in polymer particles, in g-mole/l.
t = reaction time, in sec or min
X_M = monomer conversion
ρ = density of polymer particle, in g/cc
ϕ = monomer weight fraction in polymer particle
ϵ = k_2M_m/k_1
σ = surface tension, in dyne/cm

Subscripts

c = critical or constant value
0 = initial condition

One of the authors (M. Harada) wishes to thank the Sakko Kai Foundation for their (financial) support. The authors wish to express their thanks to Prof. Magari for allowing them to use the electronmicroscope in his laboratory, and to Mr. Miyoshi and Mr. Nakagawara for carrying out the experimental work.

References

1. W. V. Smith and R. H. Ewart, *J. Chem. Phys.*, **16**, 592 (1948).
2. W. D. Harkins, *J. Amer. Chem. Soc.*, **69**, 1428 (1947); *J. Polym. Sci.*, **5**, 217 (1947).
3. C. P. Roe, *Ind. Eng. Chem.*, **60** (No. 9), 20 (1968).
4. A. I. Goldberg, W. P. Hohenstein, and H. Mark, *J. Polym. Sci.*, **2**, 503 (1947).
5. W. H. Stockmayer, *J. Polym. Sci.*, **24**, 314 (1957).
6. C. H. Olive and S. Olive, *Makromol. Chem.*, **37**, 71 (1960).
7. E. Bartholome, H. Gerrens, H. Herbeck, and H. M. Weitz, *Z. Elektrochem.*, **60**, 334 (1956).
8. I. M. Kolthoff and I. K. Miller, *J. Amer. Chem. Soc.*, **73**, 3055 (1951).

Received December 1, 1969
Revised July 29, 1970; October 21, 1971